Article ID: 1671-3664(2007)02-0171-11 **DOI**: 10.1007/s11803-007-0732-4

Damping characteristics of friction damped braced frame and its effectiveness in the mega-sub controlled structure system

Lian Yeda (连业达)[1†] , Zhang Xunan (张洵安)[1‡] and Sheldon Cherry[2§]

1. *College of Mechanics and Civil Engineering, Northwestern Polytechnic University, Xi'an 710072, China*
2. *Department of Civil Engineering, University of British Columbia, Vancouver, Canada*

Abstract: Based on energy dissipation and structural control principle, a new structural configuration, called the mega-sub controlled structure (MSCS) with friction damped braces (FDBs), is first presented. Meanwhile, to calculate the damping coefficient in the slipping state a new analytical method is proposed. The damping characteristics of one-storey friction damped braced frame (FDBF) are investigated, and the influence of the structural parameters on the energy dissipation and the practical engineering design are discussed. The nonlinear dynamic equations and the analytical model of the MSCS with FDBs are established. Three building structures with different structural configurations, which were designed with reference to the conventional mega-sub structures such as used in Tokyo City Hall, are comparatively investigated. The results illustrate that the structure presented in the paper has excellent dynamic properties and satisfactory control effectiveness.

Keywords: friction damped braces; mega-sub controlled structure; energy dissipation; vibration control; nonlinear dynamic system

1 Introduction

As buildings in many large cities are taller, more attention is focused on their structural safety against extreme loads such as earthquakes and typhoons and on the effect of daily random wind loads. However, the safety and degree of comfort etc. are still a serious challenge for the researchers and designers in design and construction of super- and extremely super- tall buildings. In recent years, some new methods to reduce structural responses have been proposed and discussed, among them the Friction Damped Braced Frame (FDBF) and the Mega-Sub Controlled Structure (MSCS) systems could be two of the most noticeable methods. FDBF is based on a novel Friction Damper (FD) device, originally proposed by Pall and March (1982), when they designed an FD and located it at the crossing of two braces, where tension in one of the braces forces the joint to slip thus activating four links, which in turn force the joint in other brace to slip. Filiatrault *et al*. (1988) made an improvement in which the FD slips at an optimum predetermined force, which allows the structure to mechanically dissipate the input seismic energy by its hysteretic effect rather than by inelastic deformation of the structural elements. The improved FD device had been successfully applied to some practical structures. Another kind of FD device, which was proposed by Grigorian and Popov (1993), utilizes slotted bolt connection (SBC) as the braced connection, which is basically composed of high strength bolts to connect the two parts of the brace with slotted holes and thin alloy plates inserted between the gusset and splice plates, and is relatively easy to be constructed and implemented by using only commercially available materials. All these indicate that FD is greatly attractive for its use in the seismic design of both new buildings and the retrofit of existing structures.

The idea of a MSCS system was first advanced by Chai and Feng (1997), and its design is based on the control principle of tuned mass damper (TMD) to form a self-controlling structural system. More recently, an improved practical MSCS was proposed by Zhang *et al*.(2004a and b). This research has shown that the improved MSCS system can provide a large amount of energy for control and is very effective in reducing structural displacement and acceleration responses.

Basing on the improved MSCS system and energy dissipation and structural control principles, this paper presents a new structural configuration, in which Friction Damped Braces (FDBs) are incorporated in a sub-frame of a MSCS system. The new structural configuration

Correspondence to: College of Mechanics and Civil Engineering, Northwestern Polytechnic University, Xi'an 710072, China
Tel: 13468850314
E-mail: lianyeda@163.com
[†]PhD Candidate; [‡]Professor; [§]Emeritus Professor

Supported by: Science and Technology Fund of NWPU Under Grant No. M450211 and Seed Fund of NWPU Under Grant No. Z200729
Received April 9, 2007; **Accepted** May 14, 2007

is called a MSCS system with FDBs. A new method is proposed to evaluate the damping coefficient of the FDBF which differs from the equivalent damping and equivalent linear method adopted by Dowdell and Cherry (1994) and Fu and Cherry (1999). Though the latter method is simple, it does not accurately describe some important dynamic properties. To illustrate the vibration control effectiveness of the proposed MSCS system with FDBs, numerical comparisons are made among the seismic responses of three different buildings designed with different structural configurations.

2 Damping characteristic of one-storey FDBFs

2.1 Dynamic equations of structures with FDBs and their solution

To investigate the FD performance, such as the amount of slipping displacement, slipping time and the energy dissipation in terms of different FD parameters, a one-storey FDBF and a corresponding analysis model is developed, as shown in Figs.1 (a) and (b), respectively, where the FD's damping c_{fd} varies over time, while the FD's friction force is approximately assumed to be a constant as FD slipping. To simplify the response analysis a mean damping value c_{fdm} is taken. Then, the corresponding dynamic equations are written as:

$$m\ddot{x} + c\dot{x} + kx + F(x,\dot{x}) = -m\ddot{x}_{\mathrm{g}} \tag{1}$$

$$F(x,\dot{x}) = \begin{cases} k_{\mathrm{fd}}x, & -\Delta_1 + \Delta_{\mathrm{s}} \le x \le \Delta_1 + \Delta_{\mathrm{s}} \\ c_{\mathrm{fdm}}\dot{x}_{\mathrm{m}}, & x < -\Delta_1 + \Delta_{\mathrm{s}} \quad \text{or} \quad x > \Delta_1 + \Delta_{\mathrm{s}} \end{cases} \tag{2}$$

where m,c and k are respectively the mass, damping and stiffness of an unbraced frame ; x is the displacement of the structure relative to its base; F is the FDB's force acting on this frame; k_{fd} is FDB's stiffness; c_{fdm} and $\dot{x}_{\mathrm{m}}$ are the FD's mean damping value and mean slipping velocity, respectively, when FD device is in the slipping state; and Δ_1 and Δ_{s} are respectively the initial starting slipping displacement and slipping displacement of FD device in FDBF(see Fig.2).

Introducing non-dimensional parameters defined as: stiffness ratio $\alpha = k_{\mathrm{fd}}/k$, damping ratio $\beta = c_{\mathrm{fdm}}/c$ and the relative starting slipping displacement ratio $\theta = \Delta_1 / \mathrm{rms}(D)$, where rms$(D)$ is the root mean squared (RMS) displacement response of the corresponding frame with common steel brace with stiffness k_{fd} . Then, the Eqs. (1) and (2) can be rewritten as:

$$\ddot{x} + 2\zeta\omega\dot{x} + \omega^2 x + F^* = -\ddot{x}_{\mathrm{g}} \tag{3}$$

$$F^* = \begin{cases} \alpha\omega^2 x, & -\theta\cdot\mathrm{rms}(D) + \Delta_{\mathrm{s}} \le x \le \theta\cdot\mathrm{rms}(D) + \Delta_{\mathrm{s}} \\ 2\zeta\omega\beta\dot{x}_{\mathrm{m}}, & x < -\theta\cdot\mathrm{rms}(D) + \Delta_{\mathrm{s}} \\ & \text{or} \quad x > \theta\cdot\mathrm{rms}(D) + \Delta_{\mathrm{s}} \end{cases} \tag{4}$$

where, ω is the natural frequency of the unbraced frame.

Combining Figs.1, 2 and 4, in which the slipping joint structure of the FD device is incorporated, the slipping force P_{s} in the FDBF can be expressed as:

$$P_{\mathrm{s}} = k_{\mathrm{fd}}\cdot\Delta_1 = \sum \gamma\cdot N\cdot\mu\cdot\cos\varphi \tag{5}$$

where N is the normal force of the FD device; μ is the material friction coefficient for the slipping face; γ is the degrading coefficient of friction force when FD device is slipping; and φ is the slope angle from the horizontal shown in Fig.1(a).

As the total slipping length Δ_{s}^i equals $\sum_{i=1}^{n}\Delta_{\mathrm{s}}^i$, dissipated energy of the FD during the entire slipping phase is expressed as:

$$P_{\mathrm{s}}\cdot\sum_{i=1}^{n}\Delta_{\mathrm{s}}^i = \sum\int_{\Delta_{\mathrm{s}}^i} c_{\mathrm{fdm}}\dot{x}_{\mathrm{m}}\mathrm{d}x \tag{6}$$

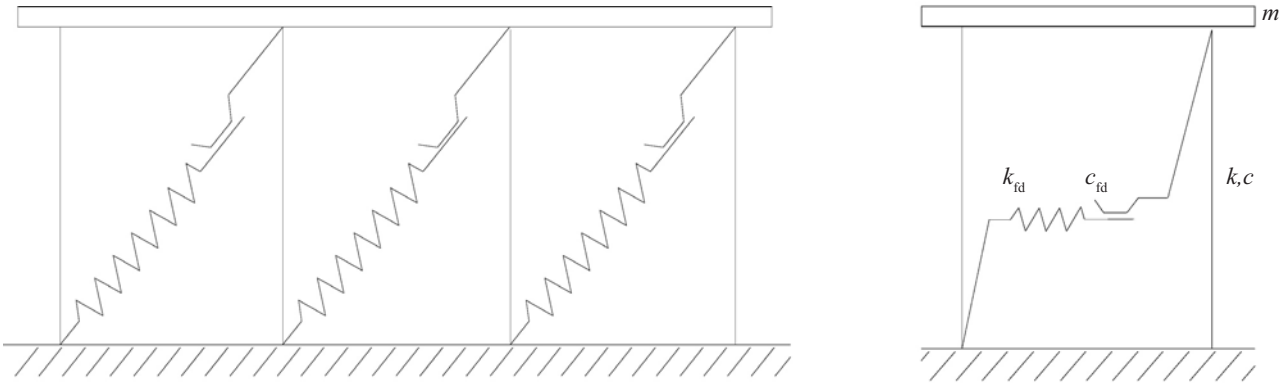

(a) One-storey FDBF (b) Analytical model

Fig. 1 One-storey FDBF and its analytical model

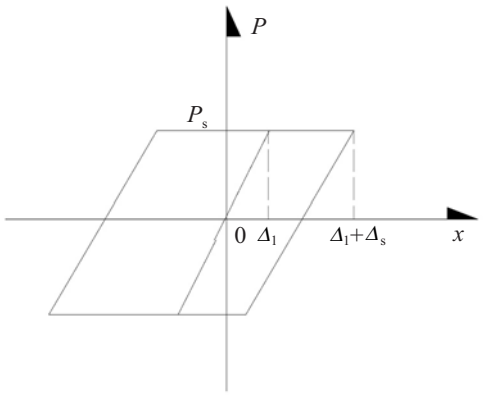

Fig. 2 Hysteresis loop of FD device

where Δ_s^i is the i^{th} slipping displacement, and $\int_{\Delta_s^i}$ is the integral in the Δ_s^i.

From Eq. (6), the damping ratio of the FD is expressed as:

$$\beta = \frac{P_s \cdot \sum(\Delta_s^i / t_s)}{2\zeta \cdot \sqrt{mk} \cdot \sigma_{\dot{x}s}^2} \tag{7}$$

where, t_s and $\sigma_{\dot{x}s}^2$ are the total slipping time and the mean square velocity response in $\sum_{i=1}^{n} \Delta_s^i$.

From Eqs. (7) and (5), it is found that as the friction force increases, the damping ratio increases,since the velocity items of (Σ (Δ_s^i / t_s)) and $\sigma_{\dot{x}s}^2$ decrease respectively and the item of (Σ (Δ_s^i / t_s))/ $\sigma_{\dot{x}s}^2$ increases, if *m, k* and ζ keep constant. This is an important characteristic, which show us the ways to further improve the FD performance. For example, the FD device can be designed by using high strength bolts to promote the normal force *N* and using high friction coefficient material, which could be embedded in the connecting plates in the slipping faces as shown in Fig. 4 to increase the μ's value, take some measure to decrease the friction force degrading while FD device is in slipping state, and install multi-FDs side by side in one storey to increase β etc. Finally, from the Eq. (5), the stiffness k_{fd} has the following expression as a certain Δ_1 is given.

$$k_{fd} = \gamma \cdot N \cdot \mu \cdot \cos\varphi / \Delta_1 \tag{8}$$

2.2 Analysis for equations characterizing FD braced frame

As Eqs. (3), (4) and (7) represent motions of a complex nonlinear dynamic system with hysteresis loops as illustrated in Fig. 2, it is difficult to directly obtain analytical expressions of the RMS displacement and acceleration responses by the random vibration method (Zhang *et al*., 2004a and b). However, using the statistical method, the mean square displacement response σ_x^2 and acceleration response $\sigma_{\ddot{x}}^2$ can be approximately calculated, respectively, by

$$\sigma_x^2 = E[X \cdot X] \approx \frac{1}{n_1}\sum_{i=1}^{n} X_i^2$$

$$\sigma_{\ddot{x}}^2 = E[\ddot{X} \cdot \ddot{X}] \approx \frac{1}{n_1}\sum_{i=1}^{n_1} \ddot{X}_i^2 \tag{9}$$

with $$X_i = \frac{1}{n_2}\sum_{j=1}^{n_2} x_{i,j} \qquad \ddot{X}_i = \frac{1}{n_2}\sum_{j=1}^{n_2} \ddot{x}_{i,j} \tag{10}$$

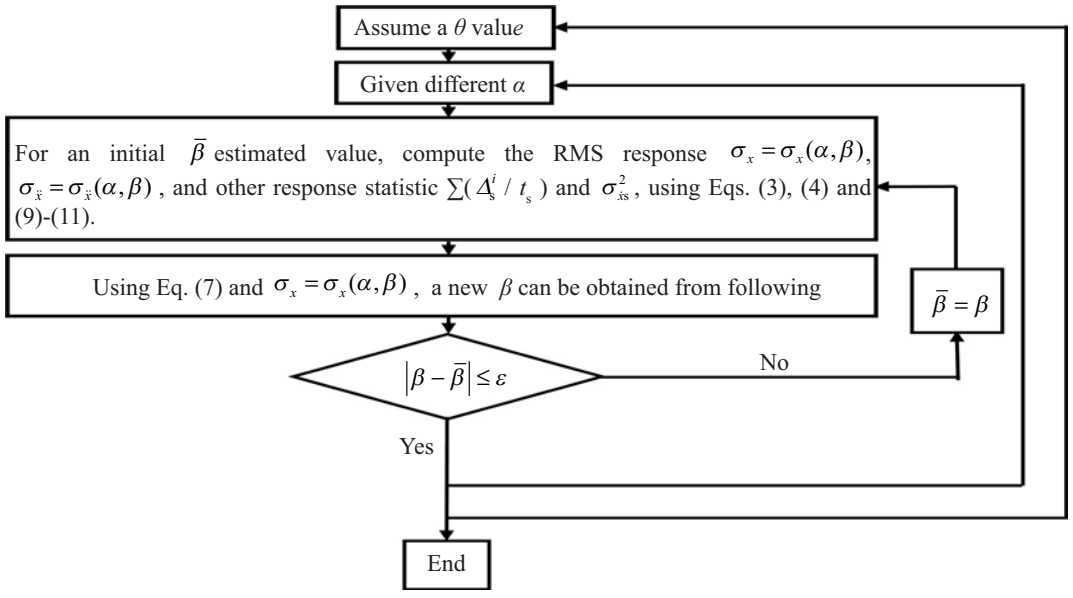

Fig. 3 Flow chart for damping ratio calculation of FDBs

where X_i and $\ddot{X}_i$ are, respectively, the displacement and acceleration statistical mean value of all samples as $t=t_i$; $x_{i,j}$ and $\ddot{x}_{i,j}$ are, respectively, the j^{th} displacement and acceleration response samples, as $t=t_i$; n_1 is the total number of the time steps and n_2 is the total number of samples.

The calculation of the damping ratio, β, can be conducted by following the steps in the flow chart.

In the above analysis the selection of the seismic excitation samples is an important step, as they should include different frequency characteristics of ground motions. Without losing generality, it is better to take the white noise time histories with unit peak as the ground acceleration samples. Their expressions can be simulated as:

$$\ddot{x}_g(t)=\frac{\sqrt{s_0}}{\max\left|\ddot{x}_g\right|}\sum_{k=1}^{N}\sqrt{2\cdot\Delta\omega_k}\left[\cos(\omega_k\cdot t+\varphi_k)\right] \qquad (11)$$

where s_0 is the spectrum density of the white noise; N is a large integer number; φ_k is a uniformly distributed random function in [0, 2π]; $\Delta\omega_k=(\omega_N-\omega_L)/N$ and $\omega_k=\omega_L+(k\text{-}1/2)\Delta\omega_k$, ($k$=1,2,3……$N$), where ω_L and ω_N denote the frequency lower and upper bounds, respectively. One of these samples is represented in Fig. 5.

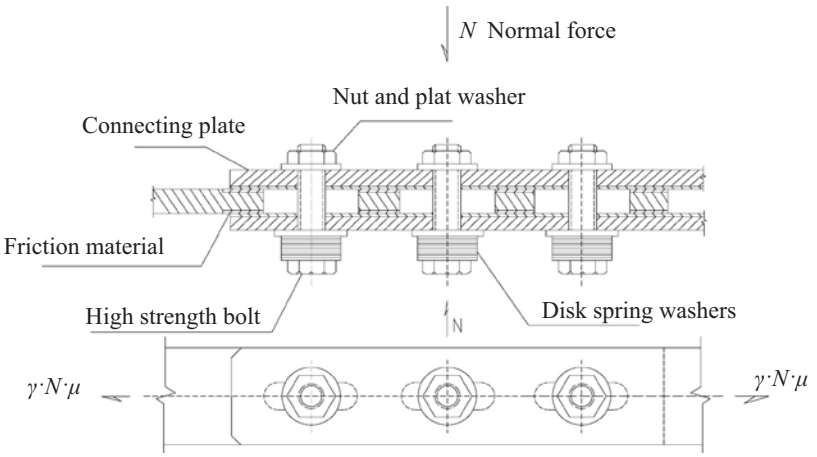

Fig. 4 Slipping joint structure of FD device

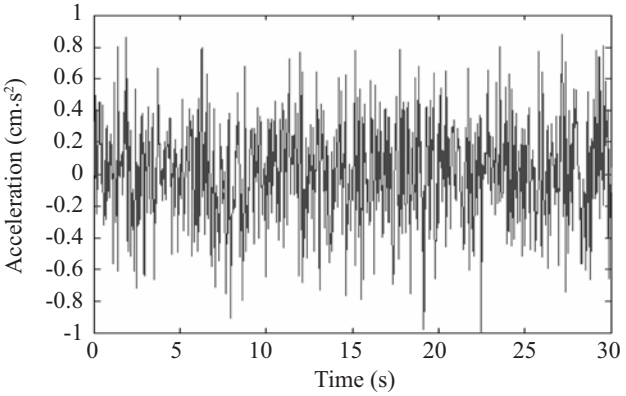

Fig. 5 A sample of ground excitation

2.3 FDBF vs common braced frame without FDs

Figure 6 further presents a comparison of the RMS displacement and acceleration responses to white noise defined in the above section for a one-storey FDBF shown in Fig. 1(a) and a common steel braced frame, when the relative starting slipping displacement ratio θ=50%. It clearly shows the satisfactory effectiveness and the working property of the FD device. The damping ratio variation with the stiffness ratio α is plotted in Fig. 7.

Table 1 further gives the effect of the stiffness ratio α and the relative starting slipping displacement ratio θ on the damping ratio β and the RMS displacement / acceleration response ratios between the FDBFs and frames with common steel braces. Note that, with increasing θ the damping ratio β increases for all values of α considered. However, the dependence of the response ratio on $\alpha,\theta(\beta)$ is more complicated. With increasing θ the response ratio increases for α=0.5, but decreases for α=0.6, and it takes a minimum value for a medium θ (=0.5) It means that in this time the FDBF has a longer slipping distance so that it still has good energy dissipation ability though the damping ratio is larger than other θ values.

3 The MSCS with FDBs and its dynamic equations

Taking the advantage of the damping characteristics of the FDBF discussed above, the MSCS system with FDBs, a new structural configuration is developed in this section.

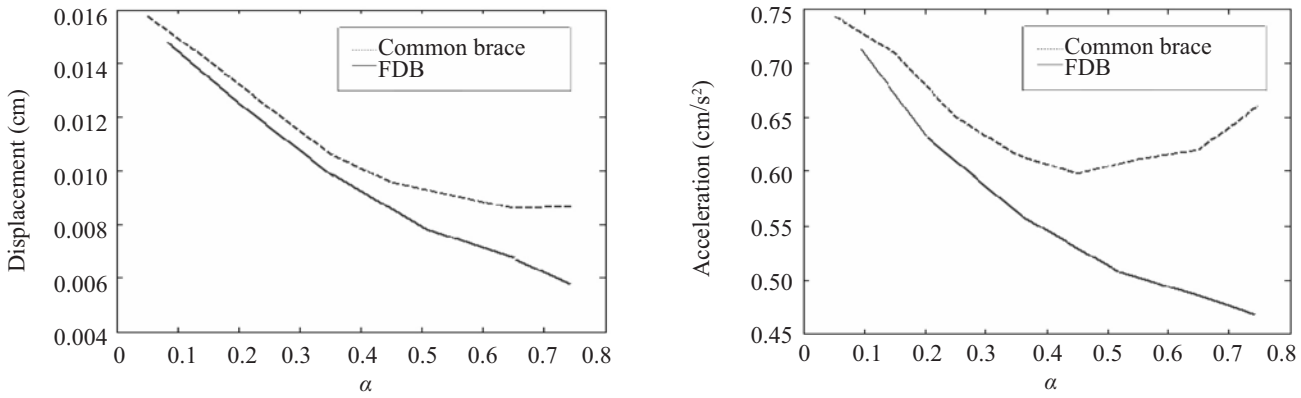

(a) Displacement response (b) Acceleration response

Fig. 6 The comparison of root mean squared responses between FDBF (solid lines) and the common brace frame (dashed lines) with different stiffness ratio α, while $\theta = 0.5$

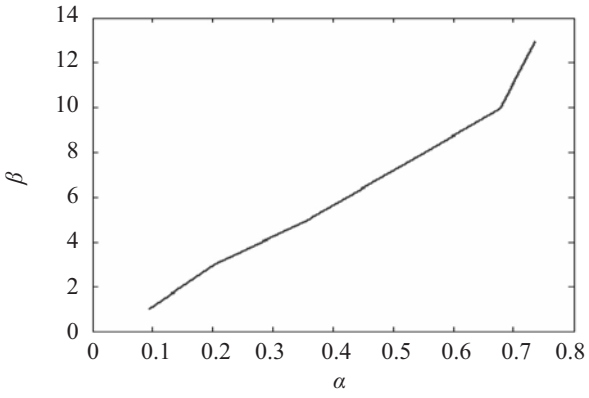

Fig. 7 Variety of damping ratio β with stiffness ratio α, while $\theta = 0.5$

3.1 Configuration of the MSCS system with FDBs

The MSCS configuration is constructed by rebuilding a conventional mega-sub structure, which consists of two major components—a mega-frame, which is the main structural frame of the building, and several sub-frames, each of which may contain several floors used for residential and/or commercial purposes, as shown in Fig. 8(a). In conventional mega-sub structure design, sub-frames are rigidly connected with the mega-frame, while the MSCS system exhibits relative isolated sub-frames, which can effectively suppress the vibration of the entire building since they benefit from the reciprocity between the mega-frame and sub-frames. An improved practical MSCS configuration ever proposed by Zhang *et al*. (2004a and b) is shown in Fig. 8(b), where the sub-frames are combined with some viscous dampers installed between the mega-frame and sub-frames. They are designed to form a huge mass damper to control the entire range of structural responses, instead of using the base isolation for the sub-frame as proposed by Lan *et al*. (2002), and some additional columns are introduced to improve the over-large span of the mega beams and mega-beam-floor structures. This improved MSCS configuration, however, is more advantageous than the common tuned mass damper (TMD) system. First, no additional mass is needed and the hidden safety concerns regarding with the TMD device for tall and super tall buildings is eliminated. Second and more importantly, the mass ratio between the sub-and mega-frames is much higher (as high as 100%) than that in the common TMD system (usually 1%-5%), so that the MSCS system possesses a much larger vibration absorption capability. To achieve a further enhancement of control effectiveness in reducing structural responses, based on the above MSCS system an improved configuration is developed as shown in Fig. 8(c) where the FDBs are incorporated in the sub-frames.

Table 1 Damping ratio β and the RMS displacement / acceleration response ratio

θ	α					
	0.5		0.6		0.7	
	β	Response ratio	β	Response ratio	β	Response ratio
0.35	5.8	0.8473/0.8432	6.3	0.8278/0.8153	8.2	0.7588/0.7644
0.5	7.1	0.8577/0.8525	8.3	0.8068/0.7902	11.0	0.7120/0.7460
0.6	8.5	0.8787/0.8549	11.0	0.7609/0.7721	13.0	0.7327/0.7602

Note: Numerals on the left and the right of the slant represent the displacement and acceleration response ratio, respectively.

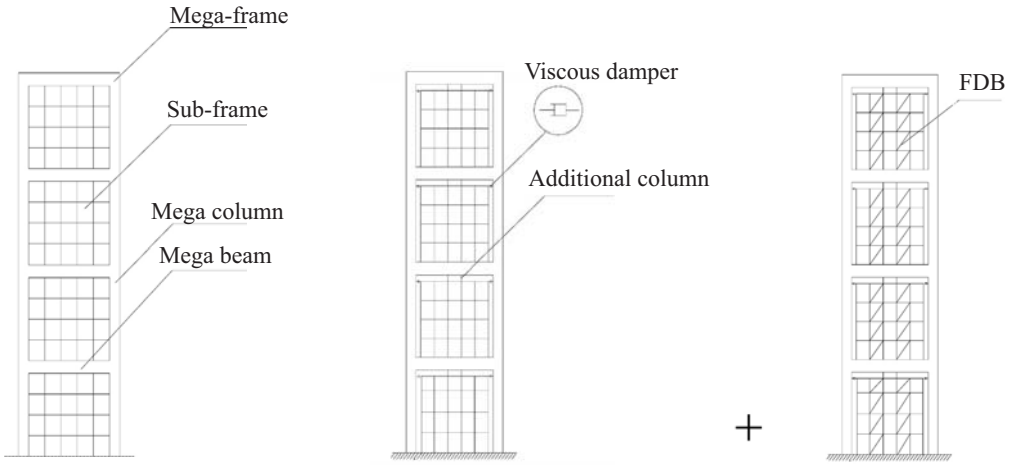

(a) Conventional mega-sub structure (b) MS controlled structure (c) MS controlled structure with FDBs

Fig. 8 Different structural configurations

3.2 Analytical model and dynamic equations

The new MSCS system with FDBs is modeled as a MDOF system, as shown in Fig.9, where it is assumed that bending is the dominant vibration mode for the mega-frame, while shear is the governing mode for the sub-frames, since the sub-frames are usually not slender. Suppose there are n mega-floors and n_1 relatively isolated sub-frames, each of which consists of n_z floors, the total DOF number of this structure is $N_1=n+n_1\times n_z$. Hence, the dynamic equation under the ground excitation is expressed as:

$$\boldsymbol{M}\ddot{\boldsymbol{X}}+\boldsymbol{C}\dot{\boldsymbol{X}}+\boldsymbol{K}\boldsymbol{X}+\boldsymbol{F}_{\mathrm{d}}=-\boldsymbol{M}^{*}\ddot{x}_{\mathrm{g}} \tag{12}$$

where, $\boldsymbol{X}=[\boldsymbol{x}_{\mathrm{p}}{}^{\mathrm{T}},\boldsymbol{x}_{1}{}^{\mathrm{T}},\boldsymbol{x}_{2}{}^{\mathrm{T}},.....,\boldsymbol{x}_{n_1}{}^{\mathrm{T}}]^{\mathrm{T}}$ is the deformation vector of the building with N_1 variables, and $\mathbf{x}_{\mathrm{p}}^{\mathrm{T}}=[x_{\mathrm{p},1},x_{\mathrm{p},2},\cdots,x_{\mathrm{p},n}]^{\mathrm{T}}$ and $\boldsymbol{x}_{i}^{\mathrm{T}}=[x_{i,1},x_{i,2},\cdots,x_{i,n_z}]^{\mathrm{T}}$

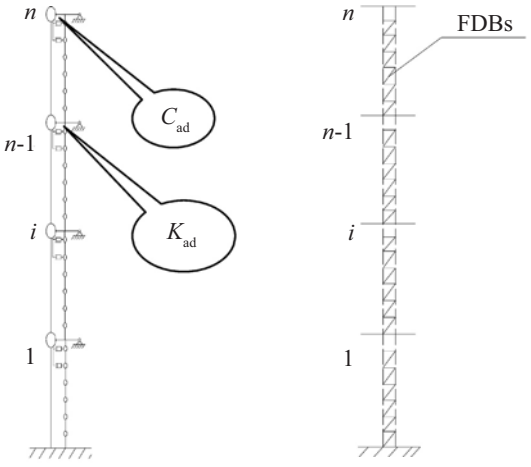

(a) Main structure (b) The location of FDBs

Fig. 9 Analytical model for proposed MSCF with FDBs

(i=1,2,…, n_1) are the deformation vectors of the mega-frame and the i^{th} sub-frame, respectively; $\boldsymbol{M}^{*}$is the mass vector; $\ddot{x}_{\mathrm{g}}$ is the random seismic acceleration; and $\boldsymbol{F}_{\mathrm{d}}$ is the force vector supplied by friction damping devices.

● The expression of the force vector $\boldsymbol{F}_{\mathrm{d}}$

The force vector $\boldsymbol{F}_{\mathrm{d}}$ has the following form:

$$\begin{aligned}\boldsymbol{F}_{\mathrm{d}}=\{&[f_{\mathrm{p}1},...,f_{pi},...,f_{pn}]^{\mathrm{T}},[f_{1,1},...,f_{1,j},...,f_{1,n_Z}]^{\mathrm{T}},...,\\&[f_{i,1},...,f_{i,j},...,f_{i,n_Z}]^{\mathrm{T}},...,[f_{n_1,1},...,f_{n_1,j},...,f_{n_1,n_{\mathrm{Z}}}]^{\mathrm{T}}\}^{\mathrm{T}}\end{aligned} \tag{13}$$

where the element f_{pi} can be expressed as:

$$f_{\mathrm{p}i}=\begin{cases}\alpha_{i+1,1}\cdot k_{i+1,1}(x_{\mathrm{p}i}-x_{i+1,1}),\\ \quad -\Delta^{1}_{i+1,1}+\Delta^{\mathrm{s}}_{i+1,1}\le x_{\mathrm{p}i}-x_{i+1,1}\le\Delta^{1}_{i+1,1}+\Delta^{\mathrm{s}}_{i+1,1}\\ \beta_{i+1,1}\cdot c_{i+1,1}(\dot{x}_{\mathrm{p}i}-\dot{x}_{i+1,1}),\ x_{\mathrm{p}i}-x_{i+1,1}<-\Delta^{1}_{i+1,1}+\Delta^{\mathrm{s}}_{i+1,1},\\ \quad \text{or}\quad x_{\mathrm{p}i}-x_{i+1,1}>\Delta^{1}_{i+1,1}+\Delta^{\mathrm{s}}_{i+1,1}\end{cases}$$
$$f_{\mathrm{p}n}=0 \tag{14}$$

And the element in Eq. (13) can be further decomposed into:

$$f_{i,j}=f^{\mathrm{d}}_{i,j}+f^{\mathrm{u}}_{i,j} \tag{15}$$

$$f^{\mathrm{d}}_{i,j}=\begin{cases}\alpha_{i,j}\cdot k_{i,j}(x_{i,j}-x_{i,j-1}),\\ \quad -\Delta^{1}_{i,j}+\Delta^{\mathrm{s}}_{i,j}\le x_{i,j}-x_{i,j-1}\le\Delta^{1}_{i,j}+\Delta^{\mathrm{s}}_{i,j}\\ \beta_{i,j}\cdot c_{i,j}(\dot{x}_{i,j}-\dot{x}_{i,i-1}),\ x_{i,j}-x_{i,j-1}<-\Delta^{1}_{i,j}+\Delta^{\mathrm{s}}_{i,j}\\ \quad \text{or}\ \ x_{i,j}-x_{i,j-1}>\Delta^{1}_{i,j}+\Delta^{\mathrm{s}}_{i,j}\end{cases}$$
$$i=1,2,3,.....,n_1;\quad j=1,2,3,.....,n_z \tag{16}$$

$$f_{i,j}^{\mathrm{u}}=\begin{cases}\alpha_{i,j+1}\cdot k_{i,j+1}(x_{i,j}-x_{i,j+1}), \\ -\Delta_{i,j+1}^{1}+\Delta_{i,j+1}^{s}\le x_{i,j}-x_{i,j+1}\le\Delta_{i,j+1}^{1}+\Delta_{i,j+1}^{\mathrm{s}} \\ \beta_{i,j+1}\cdot c_{i,j+1}(\dot{x}_{i,j}-\dot{x}_{i,i+1}), \quad x_{i,j}-x_{i,j+1}<-\Delta_{i,j+1}^{1}+\Delta_{i,j+1}^{\mathrm{s}} \\ \text{or} \quad x_{i,j}-x_{i,j+1}>\Delta_{i,j+1}^{1}+\Delta_{i,j+1}^{\mathrm{s}}\end{cases}$$
$$i=1,2,3,...,n_1;\quad j=1,2,3,...,n_z \tag{17}$$

where $\alpha_{i,j}=k_{f\mathrm{di},j}/k_{i,j}$ and $\beta_{i,j}=c_{\mathrm{fdi},j}/c_{i,j}$ are respectively the stiffness ratio and damping ratio; $k_{\mathrm{fd}i,j}$ and $c_{\mathrm{fd}i,j}$ are the stiffness and damping of the FDB, respectively; $k_{i,j}$ and $c_{i,j}$ are respectively the stiffness and damping of the i^{th} sub-frame on its j^{th} floor; $\Delta_{i,j}^{\mathrm{s}}$ and $\Delta_{i,j}^{1}$ are respectively the slipping displacement and the starting slipping displacement of the FD device on the j^{th} floor of the i^{th} sub-frame. Here, $\Delta_{i,j}^{1}=\theta_{i,j}\cdot\mathrm{rms}(D_{i,j})$, where rms ($D_{i,j}$) are defined as the RMS displacement response on the j^{th} floor of the i^{th} sub-frame with common braces whose stiffness equals $k_{\mathrm{fd}i,j}$, and $\theta_{i,j}$ is the corresponding displacement ratio.

● The expression of mass matrix

The mass matrix $\boldsymbol{M}$ in Eq.(12) can be expressed as:

$$\boldsymbol{M}=\mathrm{diag}\,[\boldsymbol{M}_{\mathrm{p}},\boldsymbol{M}_1,\boldsymbol{M}_2,\cdots\boldsymbol{M}_i\cdots,\boldsymbol{M}_{n_1}] \tag{18}$$

where $\boldsymbol{M}_{\mathrm{p}}$ is the $n\times n$ diagonal mass matrix of the mega-frame, and M_i (i=1,2,…,n_1) is the $n_z\times n_z$ diagonal mass matrix of the i^{th} sub-frame.

● The expression of stiffness matrix

The stiffness matrix in Eq.(12) can be written as:

$$\boldsymbol{K}=\begin{bmatrix}\boldsymbol{K}_{\mathrm{p}}+\boldsymbol{K}_{\mathrm{s,diag}} & \boldsymbol{K}_{\mathrm{c}} \\ \boldsymbol{K}_{\mathrm{c}}^{\mathrm{T}} & \boldsymbol{K}_{\mathrm{s}}\end{bmatrix}$$

$$\boldsymbol{K}_{\mathrm{s}}=\mathrm{diag}\,[\boldsymbol{K}_{\mathrm{s},1},\boldsymbol{K}_{\mathrm{s},2},\cdots,\boldsymbol{K}_{\mathrm{s},i},\cdots,\boldsymbol{K}_{\mathrm{s},n_1}] \tag{19}$$

where K_{p} is the $n\times n$ stiffness matrix of the mega-frame, $\boldsymbol{K}_{\mathrm{s},i}$ (i=1,2,…,n_1) is the $n_z\times n_z$ stiffness matrix of the i^{th} sub-frame, and $\boldsymbol{K}_{\mathrm{s,diag}}$ has the following form:

$$\boldsymbol{K}_{\mathrm{s,diag}}=\mathrm{diag}\,[k_{2,1}+k_{\mathrm{ad}},k_{3,1}+k_{\mathrm{ad}},.....,k_{i,1}+k_{\mathrm{ad}},.....,k_{n_1,1}+k_{\mathrm{ad}},0+k_{\mathrm{ad}}] \tag{20}$$

where $k_{i,1}$ (i=2,3,…,n_1) denotes the first floor's shear stiffness of the i^{th} sub-frame, and k_{ad} is the shear stiffness of additional columns.

The matrix $\boldsymbol{K}_{\mathrm{c}}$ in Eq. (19), the coupling item between the mega-frame and the sub-frames, is a $n\times n_1n_z$ matrix and its nonzero elements can be expressed as:

$$K_{\mathrm{c}}(i,j)=\begin{cases}-k_{i+1,1} & , \quad j=i\times n_{\mathrm{z}}+1, \quad i=1,2,.....,n_1-1 \\ -k_{\mathrm{ad}} & , \quad j=i\times n_{\mathrm{z}}, \qquad i=1,2,3,.....n_1\end{cases} \tag{21}$$

● The expression of damping matrix

The damping matrix $\boldsymbol{C}$ in Eq.(12) can be expressed as:

$$\boldsymbol{C}=\begin{bmatrix}\boldsymbol{C}_{\mathrm{p}}+\boldsymbol{C}_{\mathrm{s,diag}} & \boldsymbol{C}_{\mathrm{c}} \\ \boldsymbol{C}_{\mathrm{c}}^{\mathrm{T}} & \boldsymbol{C}_{\mathrm{s}}\end{bmatrix}$$

$$\boldsymbol{C}_{\mathrm{s}}=\mathrm{diag}\,[\boldsymbol{C}_{\mathrm{s},1},\boldsymbol{C}_{\mathrm{s},2},\cdots,\boldsymbol{C}_{\mathrm{s},i},\cdots,\boldsymbol{C}_{\mathrm{s},n_1}] \tag{22}$$

where $\boldsymbol{C}_{\mathrm{p}}$ is the $n\times n$ damping matrix of the mega-frame, and $\boldsymbol{C}_{\mathrm{s},i}$ (i=1,2,…, n_1) is the $n_z\times n_z$ damping matrix of the i^{th} sub-frame.

The $n\times n_1n_z$ matrix $\boldsymbol{C}_{\mathrm{c}}$ in Eq. (22) is the coupling damping matrix between the mega-frame and the sub-frames and its nonzero elements are expressed as:

$$C_c(i,j)=\begin{cases}-c_{i+1,1}, & j=i\times n_{\mathrm{z}}+1, \quad i=1,2,.....,n_1-1 \\ -c_{\mathrm{ad}}-c_{i,n_{\mathrm{z}}+1}, & j=i\times n_{\mathrm{z}}, \qquad i=1,2,.....,n_1 \\ -c_{\mathrm{ad}}, & j=i\times n_{\mathrm{z}}-1, \quad i=1,2,3,.....,n_1\end{cases} \tag{23}$$

where $c_{i,1}$ is the first floor's damping of the i^{th} sub-frame, and c_{ad} is the additional damping contributed by viscous damper set between mega- and sub-frames. Finally, the matrix $\boldsymbol{C}_{\mathrm{s,diag}}$ in Eq. (22) can be expressed as:

$$\boldsymbol{C}_{\mathrm{s,diag}}=\mathrm{diag}\,[c_{2,1}+2\times c_{\mathrm{ad}}+c_{1,n_z+1},c_{3,1}+2\times c_{\mathrm{ad}}+c_{2,n_z+1},.....,c_{i,1}+2\times c_{\mathrm{ad}}+c_{i-1,n_z+1},.....,c_{n_1-1,1}+2\times c_{\mathrm{ad}}+c_{n_1-2,n_z+1},0+2\times c_{\mathrm{ad}}+c_{n_1-1,n_z+1}] \tag{24}$$

3.3 Control effectiveness of MSCS with FDBs

In order to study the dynamic performances and control effectiveness of the MSCS system with FDBs, three types of buildings were designed and their seismic responses were calculated. Fig. 10(a) describes the building 1, which represents a conventional mega-sub structural and has been used in some actual buildings, such as Tokyo City Hall. Building 2 shown in Fig. 10(b) is an MSCS system consisting of two relatively isolated sub-frames, which was designed based on building 1. Chai and Feng (1997) and Zhang *et al*. (2004a and b) indicated that this MSCS configuration has better control effectiveness than the traditional mega-sub structure. Building 3 (see Fig. 10(c)) is a new MSCS configuration, which consists of common steel braces as in the traditional MSs on the ground sub-frame and differs from building 2 in installing FDBs on the two relatively isolated sub-frames. To ensure that these three buildings have the

same structural members and the same amount of total structural mass, some common steel braces, which have the same stiffness as the non-slipped FDBs in building 3, were added into buildings 1 and 2, as shown in Figs. 10(a) and (b). Detailed comparisons of constructional characteristic of these three buildings are presented in Table 2.

For convenience, stiffness ratio γ_K, damping ratio γ_C and mass ratio γ_M are introduced and defined, respectively, as follows:

$$\gamma_K = \frac{K^*_{sub}}{K^*_{mega}}, \quad \gamma_C = \frac{C^*_{ad}}{C^*_{sub}}, \quad \gamma_M = \frac{M_{sub}}{M_{mega}} \tag{25}$$

where, K^*_{sub}, assumed as a variable in the following text, is shear stiffness of the sub-frame; K^*_{mega}, assumed as a constant, is the bending stiffness of the mega-frame; c^*_{ad} is damping of the viscous damper set between the mega-frame and sub-frame; c^*_{sub} is sub-frame's story-damping; M_{mega} is the mega-frame's total mass including the mass of the ground sub-frame; and M_{sub} is the sum mass of the two relatively isolated sub-frames.

In the following investigation, γ_M =1.187 and γ_C = 1.3, corresponding to the original design of this steel passive mega-sub-controlled frame, are adopted, while γ_K is a variable with K^*_{sub} changing values.

The parameters of the FD device are taken as $\alpha_{i,j} = \alpha$, $\beta_{i,j} = \beta$ and $\theta_{i,j} = \theta$ .. In the following ansysis, since buildings 1 and 2 are linear dynamic systems, Zhang *et al.*(2005a and b) used the complex mode analysis method of random vibration to analyze of the RMS displacement and acceleration responses under white noise and the modulated white noise excitations. However, since building 3 is a MDOF nonlinear dynamic system with hysteresis loops, both the time historic analysis and statistic analysis under the white noise sample excitations with unit peak were performed, using the Runge-Kutta method and Eq. (11) to obtain white noise time history samples.

To verify the control effectiveness of the MSCS with common braces Fig.11 presents the results of displacement and acceleration response ratios between buildings 2 and 1 with different relative stiffness ratios γ_K, while the mega-frame's fundamental period is T_m= 0.7196s. Note that the structural displacement and acceleration response ratios will correspondingly alter as the γ_K varies, and that satisfactory control effectiveness could be achieved when γ_K=0.1-0.25.

Further, to verify the control effectiveness of the MSCS with FBDs the calculated RMS response ratios between building 3 and building 2 for different α and θ are listed in Table 3. It shows that the control effectiveness of the MSCS system with FBDs can be further improved as γ_K=0.11. In fact, incorporating FBDs leads to a decrease in responses of both the sub-frames and the mega-frame. Moreover, building 3 exhibits excellent control effectiveness whether for θ=0.65 or

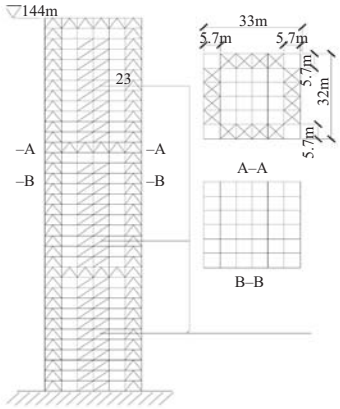

(a) Conventional steel MS structure with common braces

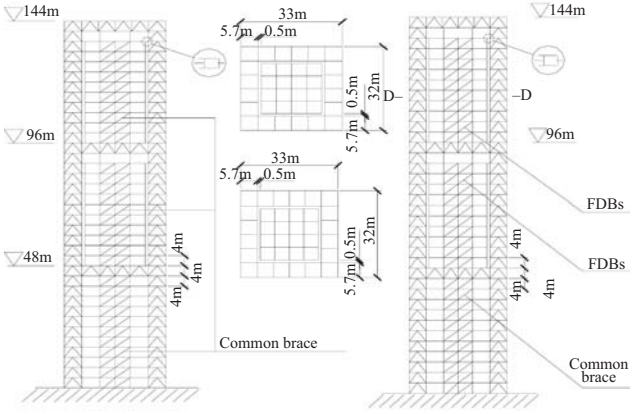

(b) Mega-sub controlled structure

(c) Steel MS controlled structure with FD braces

Fig. 10 Structural configurations of three buildings

Table 2 The characteristic comparison of three buildings

Building	Total mass	Main structural members	Brace stiffness	Isolated sub-frames	Friction damper
1	Same	Same	Same	No	No
2				Yes	No
3				Yes	Yes

θ=0.35, which is the same as the one-storey system. It is worth noting that the control effectiveness of the MSCS system with FDBs changes with the relative stiffness ratio changes, as can be seen from Table 3, where the results for γ_K=0.17 are also listed. Calculated results, which are not provided here due to limited space, show that the variation of the response ratios vs. stiffness ratio is similar with that presented in Fig. 11, and that the optimum γ_k values for buildings 2 and 3 are approximately equal.

Demonstration of a much better vibration control efficiency of the MSCS with FDBs is seen in Table 4, where results of comparison of RMS response ratios between the buildings 3 and 1 are shown.

In addition, comparisons of time history responses between buildings 3 and 1 subjected to the LANDERS

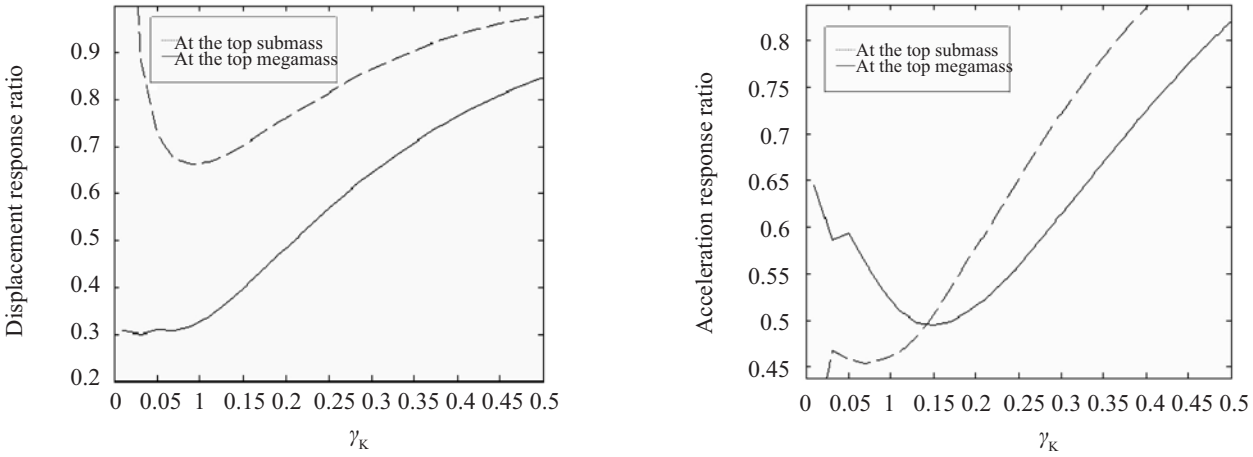

(a) Displacement response ratio (b) Acceleration response ratio

Fig. 11 Response ratios between buildings 1 and 2 with different γ_K (for T_m= 0.7196 s)

Table 3 Comparison of RMS response ratios between the buildings 3 and 2

Response	γ_K=0.11			γ_K=0.17		
	θ=0.35	θ=0.5	θ=0.65	θ=0.35	θ=0.5	θ=0.65
Displacement response at the top mega-frame	0.8258	0.8003	0.7908	0.8897	0.8231	0.8139
Displacement response at the top sub-frame	0.8023	0.7511	0.7256	0.8809	0.7717	0.7523
Acceleration response at the top mega-frame	0.8636	0.8539	0.8326	0.8841	0.8782	0.8675
Acceleration response at the top sub-frame	0.7837	0.7912	0.7901	0.8093	0.8192	0.8217

Table 4 Comparison of RMS response ratios between buildings 3 and 1

Response	γ_K=0.11			γ_K=0.17		
	θ=0.35	θ=0.5	θ=0.65	θ=0.35	θ=0.5	θ=0.65
Displacement response at the top mega-frame	0.1638	0.1383	0.1289	0.3213	0.2547	0.2455
Displacement response at the top sub-frame	0.4725	0.4213	0.3559	0.6119	0.5027	0.4833
Acceleration response at the top mega-frame	0.3683	0.3586	0.3374	0.3818	0.3759	0.3652
Acceleration response at the top sub-frame	0.2533	0.2608	0.2597	0.3397	0.3496	0.3521

waves as shown in Fig. 12 are plotted in Fig. 13. The FD's hysteresis loop of the 7th floor in the second sub-frame is presented in Fig. 14, which directly reflects the FD's working state.

Finally, note that in the analysis, the stiffness of the additional columns was taken as one fourth of the floor shear stiffness of the sub-frame, which is large enough to overcome the large span difficulty of the mega-beam floor, as has been discussed by Zhang *et al.* (2004a and b). Therefore, the MSCS system with FDBs is an excellent structural system with rational structural configuration and obvious control effectiveness.

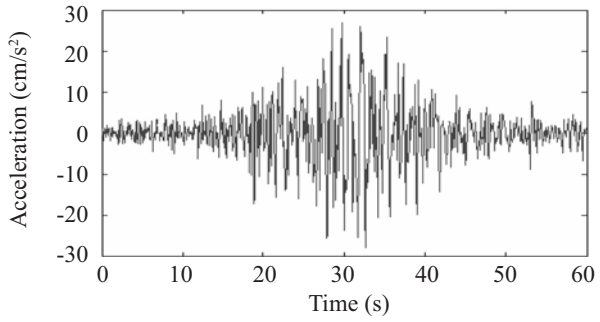

Fig.12 Acceleration time histries of Landers waves

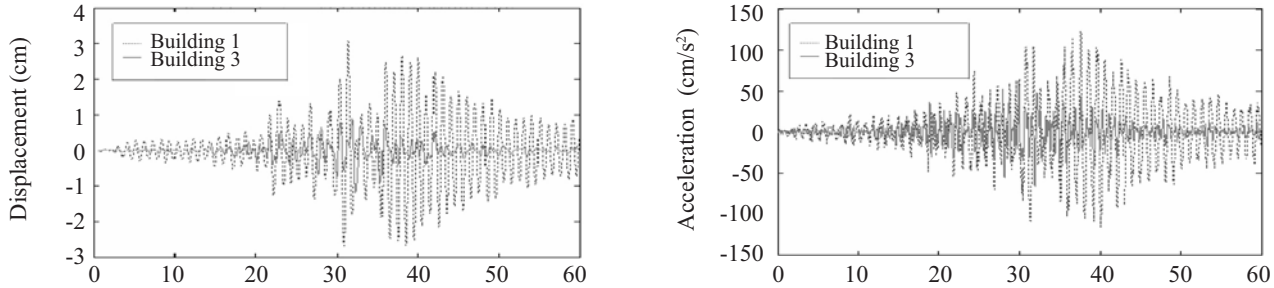

(a) Displacement responses (b) Acceleration responses

Fig. 13 Comparisons of acceleration response at the top mega mass between building 3 and building 1

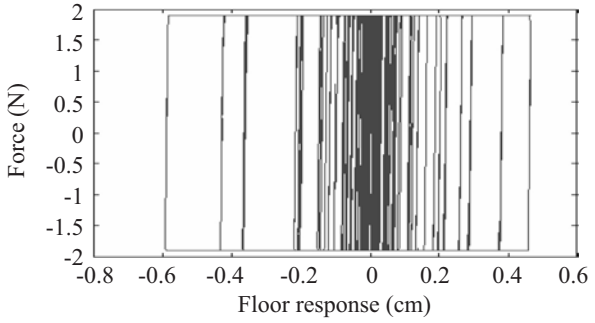

Fig.14 Hysteresis loop of the 7th floor in the second sub-frame

4 Conclusions

Friction damping braced frame (FDBF) and mega-sub controlled structure (MSCS) system respectively represent new developments in structural design, which offer some new concepts and new opportunities in the earthquake resistant design of buildings. The MSCS system with FDBs proposed first in this paper represents a new structural configuration, which combines the advantages of both FDBF and MSCS system and employs the ideas of energy dissipation and structural control to ensure structural safety against earthquakes and other dynamic loadings. These results of the present study show that the optimum response ratios of this new structural system could reach 12.89% for the RMS displacement response and 25.97 % for the RMS acceleration response, compared to a traditional MS structure, under the white noise excitation. All these explain the effectiveness and the advantages of this new structural system in earthquake design. It is concluded that incorporating FDs could effectively improve the aseismic capability of the MSCS.

In addition, the new method to calculate the FD's damping coefficient presented in this paper offers a helpful tool to simulate and analyze different FDBF by computer, such as, to investigate its practical dynamic properties, hysteresis loops, and the vibration control effectiveness. Hence, it is necessary and helpful in the practical design of FDBFs.

It should be pointed out all of the dynamic characteristics of the MSCS and FDBs and the type of seismic excitation greatly affect on the control effectiveness of MSCS with FDBs. Results of an extended study due to space limitation will be reported in another paper.

Acknowledgements

The authors would like to thank the support provided by the science and technology fund of Northwestern Polytechnical University and the seed fund of Northwestern Polytechnical University.

Reference

Chai W and Feng MQ (1997), "Vibration Control of Super Tall Buildings Subjected to Wind Loads," *Nonlinear Mechanics*, **32** (4): 657-668.

Dowdell DJ and Cherry S (1994), "Optimal Seismic Response Control of Friction Damped Structures," *Proceedings of 10th European Conference on Earthquake Engineering,* Vienna, pp.2051-2056.

Filiatrault A and Cherry S (1988), "Comparative Performance of Friction Damped Systems and Base Isolation Systems for Earthquake Retrofit and Seismic Design," *Earthquake Engineering and Structural Dynamics*, **16**: 389-416.

Filiatrault A and Cherry S (1990), "Seismic Design for Friction-damped Structures," *Journal of Structural Engineering,* ASCE, **116**(5): 1334-55.

Fu YM and Cherry S (1999), "Simplified Seismic Code Design Procedure for Friction-damped Steel Frames," Civil Engineering, **26**: 55-71.

Grigorian CE and Popov E (1993), "Slotted Bolted Connections for Energy Dissipation," *Proc Seminar on seismic Isolation, Passive Energy Dissipation, and Active Control,* Applied Technology Council, San Francisco, pp.545-556.

Lan ZJ, Fang L and Wang XD (2002), "Multifunctional Shock-absorption System of RC Megaframe Structures," *Industrial Construction*, **32** (2): 1-4. (in Chinese)

Pall AS and Marsh C (1982), "Response of Friction Damped Braced Frames," *Journal of the Structural Division*, ASCE, **108**:1313-23.

Zhang XA , Wang D and Jiang JS (2005a), "The Controlling Mechanism and the Controlling Effectiveness of Passive Mega-sub Controlled Frame Subjected to Random Wind Loads," *Journal of Sound and Vibration*, **283**: 543-560.

Zhang JL, Zhang XA and Jiang JS (2004a), "Dynamic Analysis of a Vibration Absorption System of a Mega frame via Considering the Influence of Substructure," *Proceedings of the eighth international symposium on structural engineering for young experts*, Guangzhou, pp.499-504. (in Chinese)

Zhang XA, Zhang JL and Jiang JS(2004b), "The Influence of Mega-substructural Stiffness on the Dynamic Property of the Shock-absorption-structure System of Mega-frame," *Journal of Northwestern Polythchnical University*, **22**(1):59-63. (in Chinese)

Zhang XA, Zhang JL, Wang D and Jiang JS (2005b), "Controlling Characteristics of Passive Mega-sub Controlled Frame Subjected to Random Wind Loads," *Journal of Engineering Mechanics,* ASCE, **131**(10): 1046-1055.